

## ARTICLE

# Design of Multiple Metal Doped Ni Based Catalyst for Hydrogen Generation from Bio-oil Reforming at Mild-temperature

Li-xia Yuan<sup>a,b</sup>, Fang Ding<sup>a</sup>, Jian-ming Yao<sup>a</sup>, Xiang-song Chen<sup>a</sup>, Wei-wei Liu<sup>a</sup>, Jin-yong Wu<sup>a</sup>, Fei-yan Gong<sup>b</sup>, Quan-xin Li<sup>b\*</sup>

*a. Institute of Plasma Physics, Chinese Academy Sciences, Hefei 230026, China*

*b. Anhui Key Laboratory of Biomass Clean Energy, University of Science and Technology of China, Hefei 230026, China*

(Dated: Received on November 16, 2012; Accepted on December 10, 2012)

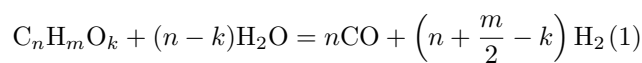
A new kind of multiple metal (Cu, Mg, Ce) doped Ni based mixed oxide catalyst, synthesized by the co-precipitation method, was used for efficient production of hydrogen from bio-oil reforming at 250–500 °C. Two reforming processes, the conventional steam reforming (CSR) and the electrochemical catalytic reforming (ECR), were performed for the bio-oil reforming. The catalyst with an atomic mole ratio of Ni:Cu:Mg:Ce:Al=5.6:1.1:1.9:1.0:9.9 exhibited very high reforming activity both in CSR and ECR processes, reaching 82.8% hydrogen yield at 500 °C in the CSR, yield of 91.1% at 400 °C and 3.1 A in the ECR, respectively. The influences of reforming temperature and the current through the catalyst in the ECR were investigated. It was observed that the reforming and decomposition of the bio-oil were significantly enhanced by the current. The promoting effects of current on the decomposition and reforming processes of bio-oil were further studied by using the model compounds of bio-oil (acetic acid and ethanol) under 101 kPa or low pressure (0.1 Pa) through the time of flight analysis. The catalyst also shows high water gas shift activity in the range of 300–600 °C. The catalyst features and alterations in the bio-oil reforming were characterized by the ICP, XRD, XPS and BET measurements. The mechanism of bio-oil reforming was discussed based on the study of the elemental reactions and catalyst characterizations. The research catalyst, potentially, may be a practical catalyst for high efficient production of hydrogen from reforming of bio-oil at mild-temperature.

**Key words:** Hydrogen generation, Bio-oil, Ni based catalyst, Mild-temperature

## I. INTRODUCTION

Currently, hydrogen production from steam reforming of bio-oil has attracted considerable attention [1]. The conventional carbonbased fossil fuels, such as coal, oil, and natural gas are becoming depleted day by day, on the other hand, hydrogen production processes from catalytic steam reforming of nonrenewable materials such as natural gas and oil-derived naphtha are accompanied by high CO<sub>2</sub> emissions, which significantly contributes to the greenhouse effect [2]. Consequently, biomass, the intriguing renewable resources could in principle be a candidate for hydrogen production [3]. Hydrogen can be produced from biomass mainly via two thermochemical processes, the gasification and the flash pyrolysis followed by steam reforming of the pyrolysis oil [4, 5]. The pyrolysis oil, known as bio-oil, generally, contains numerous and complex oxygenated organic compounds including acids, alcohols, aldehydes,

ketones, substituted phenolics and other oxygenates derived from biomass carbohydrates and lignin [6]. From an economic and environmental view, steam reforming of pyrolysis oil (bio-oil) is one of the promising routes of hydrogen production from renewable sources. The bio-oil reforming reactions would take place in the reforming reaction (Eq.(1)) or the water-gas shift reaction (WGS) (Eq.(2)) [7, 8].



During the last decade, steam reforming of bio-oil and its model compounds has been studied continuously, various catalysts such as the Ni-based catalysts (supported on such as Al<sub>2</sub>O<sub>3</sub>, MgO, CeO<sub>2</sub> and TiO<sub>2</sub> etc.) and noble metal-loaded catalysts (e.g., Pt, Ru, Rh etc.) have been selected and used for production of hydrogen from steam reforming of bio-oil and hydrocarbons [9–12]. Conventional catalysts for the steam reforming of hydrocarbons are NiO supported on a mineral (e.g., alumina, magnesia) usually operating at high temperature (600–850 °C) [8, 13]. Noble metals are gener-

\* Author to whom correspondence should be addressed. E-mail: liqx@ustc.edu.cn

ally more effective than the Ni-based catalysts and less carbon depositing but not common in real applications because of their high cost.

Lots of works on the steam reforming of bio-oil and model compounds (*e.g.*, methanol, ethanol, acetic acid *etc.*) have been extensively performed in the past [1, 14, 15], but the exorbitant reforming temperature and the catalyst deactivation still remain serious challenging in the production of hydrogen from bio-oil. The process of bio-oil reforming is much more complex than that of single organic compound. Generally, the reforming temperature to achieve a high hydrogen yield for bio-oil over a given catalyst is much higher than that of a single oxygenated organic compound, the catalyst inactivity and the reaction channels in the bio-oil reforming are much more serious and intricate than those in the reforming process of single oxygenated organic compound [7, 16]. Accordingly, developing non-noble metal catalysts suitable for the low-temperature reforming bio-oil, optimizing reforming conditions, and studying the reaction mechanism and the catalyst inactivation process are required and imperative.

In our previous work, much attention has been paid to the fast pyrolysis of biomass [9], the production of hydrogen from the volatile fraction of the bio-oil and model compounds [17, 18], and a new electrochemical catalytic reforming (ECR) bio-oil method was developed [19]. In this work, to solve the problems in hydrogen production from bio-oil, including reducing reforming temperature and deactivation of catalyst, the multiple metal doped Ni based mixed oxide catalyst was researched in electrochemical catalytic steam reforming of bio-oil. This non-noble catalyst showed good activity for reforming of bio-oil at lower operating temperature (250–500 °C) with a longer lifetime, as compared with the performance using the conventional NiO-Al<sub>2</sub>O<sub>3</sub> catalysts. The activity of water gas shift and decomposition for the oxygenated organic compounds in the bio-oil over the research catalyst, and the influences of the current on the bio-oil reforming, decomposition and catalyst microcosmic properties were studied. The mechanism of the bio-oil reforming was also discussed based on present investigations.

## II. EXPERIMENTS

### A. Catalyst preparation and characterization

The mixed oxide catalysts were prepared by the side-by-side co-precipitation method at a constant pH using respective metal nitrates as precursors and a mixture of NaOH and Na<sub>2</sub>CO<sub>3</sub> as precipitators. The main preparation procedures included: (i) preparation of respective metal nitrates solution, (ii) preparation of a mixture of NaOH (1 mol/L) and Na<sub>2</sub>CO<sub>3</sub> (1 mol/L), (iii) preparation of precipitates by the side-by-side co-precipitation of metal nitrates solution and the precipitators at a constant pH (9.0±0.5) and 80 °C, (iv)

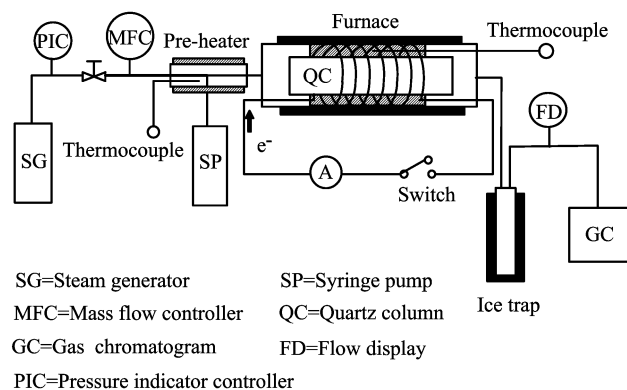


FIG. 1 Schematic setup of the fixed-bed flow reaction system for the bio-oil. ECR mode: as the Ni-Cr wire was passed through an ac electronic current for heating the catalyst and synchronously providing the electrons onto the catalyst. CSR mode: the current was shut off and the reactor was homogeneously heated by an outside furnace.

the precipitates were aged for 10 h at 25 °C, pumped and washed until pH=7, dried overnight in an oven at 110 °C, (v) then the dried precipitates were heated at 1 °C/min to 450 °C and calcined at 450 °C for 6 h in air to obtain the corresponding mixed oxide catalysts, (vi) finally, the mixed oxide catalysts were crushed into 0.1–0.2 mm and ready for the reforming.

The metallic contents in the prepared catalysts were measured by inductively coupled plasma and atomic emission spectroscopy (ICP/AES, Atom scan Advantage of Thermo Jarrell Ash Corporation, USA).

X-ray diffraction (XRD) measurements were employed to investigate the diffraction structure changes of the catalysts. XRD patterns of the catalysts were recorded on an X'pert Pro Philips diffractometer, using a Cu K $\alpha$  radiation.

The surface elements and their states were analyzed by X-ray photoelectron spectroscopy (XPS). The XPS measurements were performed on an ESCALAB-250 (Thermo-VG Scientific, USA) spectrometer with Al K $\alpha$  (1486.6 eV) irradiation source. The C1s peak at 284.6 eV was generally used as a calibration standard for determining the peaks' position and the elemental concentration.

The Brunauer-Emmett-Teller (BET) surface area and pore volume was determined by the N<sub>2</sub> physisorption at –196 °C using a COULTER SA 3100 analyzer.

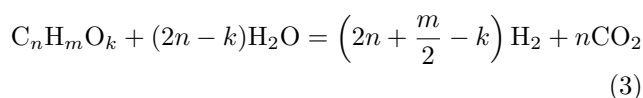
### B. Reaction system

As shown in Fig.1, the bio-oil steam reforming experiments were carried out in the continuous flow systems, using a quartz fixed-bed reactor under atmospheric pressure. The bio-oil was fed into the reactors using the multi-syringe pump (Model: TS2-60, Baoding Longer Precision Pump), the steam from a steam-generator was simultaneously fed into the reactors for

adjusting the S/C ratio (mole ratio of steam to carbon in bio-oil fed). The steam amount fed was controlled by the mass flow controller, and the effluent gases from the reactors were measured by flow display. Temperature and its distribution were measured by the thermocouples inserted into the catalyst beds. We performed the reforming experiments with following two processes, *i.e.*, the conventional steam reforming (CSR) and the ECR. For the ECR, an annular Ni-Cr wire, which passed through a given ac electronic current, entwined around a quartz column for heating the catalyst and synchronously providing the electrons onto the catalyst, and installed in the center of the reactor. The catalyst was uniformly embedded around the Ni-Cr wire. To make a certain reforming temperature, the catalyst bed was heated by a supplementary outside furnace. For the CSR, ac was shut off and the catalyst bed was homogeneously heated by an outside furnace.

The prepared bio-oil described by a chemical formula of  $\text{CH}_{2.03}\text{O}_{0.67}\cdot 0.89\text{H}_2\text{O}$  [19]. The products of the reforming reactions were analyzed by two on-line gas chromatographs (GC1 and GC2) with thermal conductivity detector (TCD). The intermediates desorbed from the catalyst surface were mass analyzed by a time-of-flight (TOF) mass spectrometer. The experimental setup of the TOF system has been described in detail elsewhere [19, 20].

The hydrogen yield was calculated as a percentage of the stoichiometric potential, in case of complete conversion of carbon element in the bio-oil to  $\text{CO}_2$  according to the reaction



The potential yield of hydrogen is  $(2n+m/2-k)$  mole per mole of carbon in the feed. The carbon conversion was calculated by the total mol carbon in the gaseous products divided by the mol carbon in the fed bio-oil. Generally, all experiments were repeated three times. The difference for each repeating, in general, ranged from zero to about 10%.

Temperature distributions in the catalyst bed under different conditions were first measured by the thermocouples inserted into different positions in the catalyst bed before running reforming test. Obviously, the temperature of the surface of Ni-Cr wire is higher than that of the near. So we have carefully detected the temperature distribution in the catalyst bed both for the ECR and the CSR in elsewhere [19]. The temperature in the center of the catalyst bed, generally, is almost close to the average value in our investigated range (250–500 °C). Generally, the averaged temperature in the catalyst bed was approximately used as the reaction temperature in the ECR and CSR experiments.

TABLE I Weight percent of metal elements in the different reforming catalysts prepared.

| Catalyst              | Metal element/% |      |      |       |       |
|-----------------------|-----------------|------|------|-------|-------|
|                       | Ni              | Cu   | Mg   | Ce    | Al    |
| Cat I: Cu-Mg-Ce-Al    | 0               | 8.20 | 6.19 | 7.43  | 37.20 |
| Cat II: Ni-Mg-Ce-Al   | 19.41           | 0    | 6.32 | 7.41  | 29.50 |
| Cat III: Ni-Mg-Cu-Al  | 19.49           | 8.29 | 6.32 | 0     | 28.80 |
| Cat IV: Ni-Cu-Ce-Al   | 18.23           | 7.63 | 0    | 6.96  | 27.00 |
| Cat V: Ni-Cu-Mg-Ce-Al | 25.95           | 5.50 | 3.72 | 11.15 | 21.29 |

### III. RESULTS AND DISCUSSION

#### A. Screening of reforming catalysts

The performance of the bio-oil reforming over various selected mixed oxide catalysts was tested under typical reforming conditions ( $T=400$  °C,  $I=0$  A,  $\text{GHSV}=10500$   $\text{h}^{-1}$ ,  $\text{S/C}=6.9$  and  $P=111.1$  kPa), shown in Table I. Figure 2 shows the carbon conversion, the yield of hydrogen, the distribution of hydrogen and various carbon-containing products over the selected catalysts. In the absence of the Ni element, the catalyst exhibited the lowest yield of hydrogen yield with the highest content of  $\text{CH}_4$ . The Ni based catalyst promoted by Cu, Ce, and Mg shows the highest reforming activity—the carbon conversion (about 60.5%) and the highest hydrogen yield (circa 58.2%) from the bio-oil reforming. In the above systems, the Ni active ingredient may play an important role in promoting C–C or C–H bonds rupture of oxygenated organic compounds, and the compositions of Cu/Ce/Mg may enhance the activity of the WGS reaction. On the other hand, adding Ce and Mg to the reforming catalysts favors to reduce the carbon-formation during the bio-oil reforming. According to present activity tests, the multiple metal doped Ni based catalyst with the atomic mole ratio of 5.6:1.1:1.9:1.0:9.9 shows the highest activity for the bio-oil reforming. Thus, much attention in this work was paid to studying the production of hydrogen from bio-oil over the above catalyst, denoted as Cat V.

#### B. Effect of current on reforming of bio-oil

In this work, the performance of the bio-oil reforming was significantly sensitive to the current  $I$  through the researched catalyst. Figure 3(a) shows dependence of the carbon conversion on  $I$  at various fixed reforming temperature. In the case of  $I=0$  (*i.e.*, CSR), the carbon conversion was very low (about 6.0%) at 250 °C, and increased to 79.8% at 450 °C. This indicates that the mixed oxide catalyst shows good low temperature reforming activity for the bio-oil. When the current passed through the catalyst (*i.e.*, ECR), however, the carbon conversion was remarkably enhanced by the current, particularly at lower temperature (250–350 °C). The carbon conversion increased from 28.3% to 84.5%

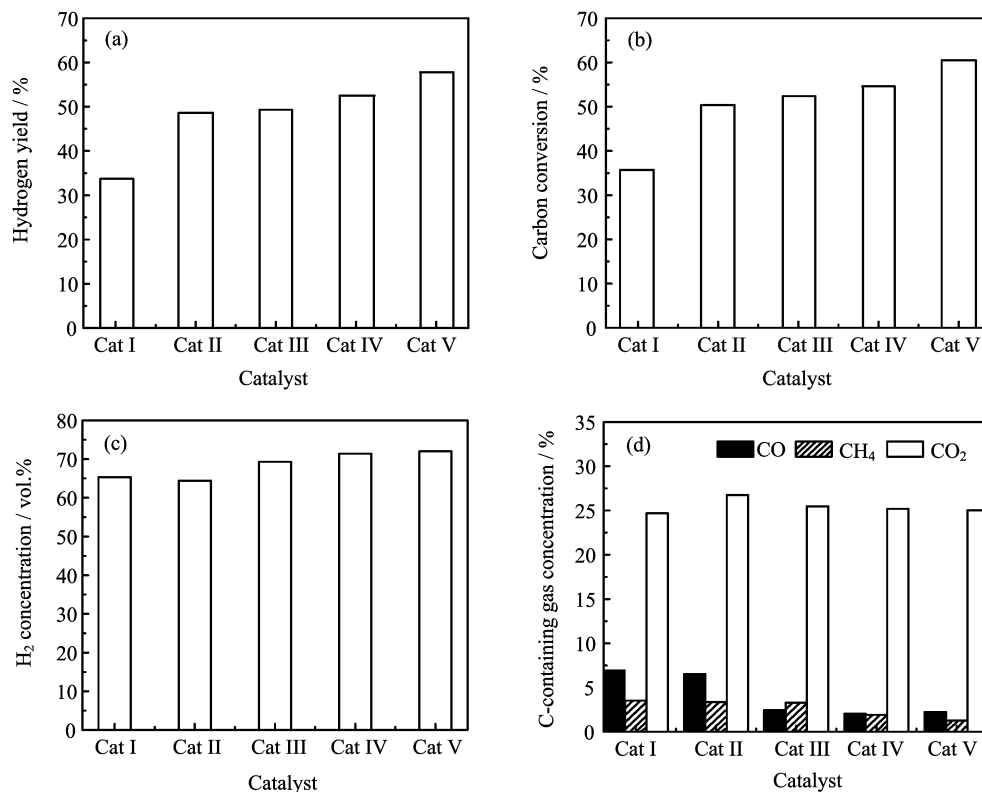


FIG. 2 The effect of the catalyst compositions on the bio-oil reforming. (a) The hydrogen yield, (b) the carbon conversion, (c) the concentration of H<sub>2</sub>, and (d) the concentration of carbon-containing gas over different catalysts respectively. Reforming conditions:  $T=400$  °C,  $I=0$  A,  $GHSV=10500$  h<sup>-1</sup>,  $S/C=6.9$  and  $P=111.1$  kPa. Cat I: Cu-Mg-Ce-Al, Cat II: Ni-Mg-Ce-Al, Cat III: Ni-Mg-Cu-Al, Cat IV: Ni-Cu-Ce-Al, Cat V: Ni-Cu-Mg-Ce-Al.

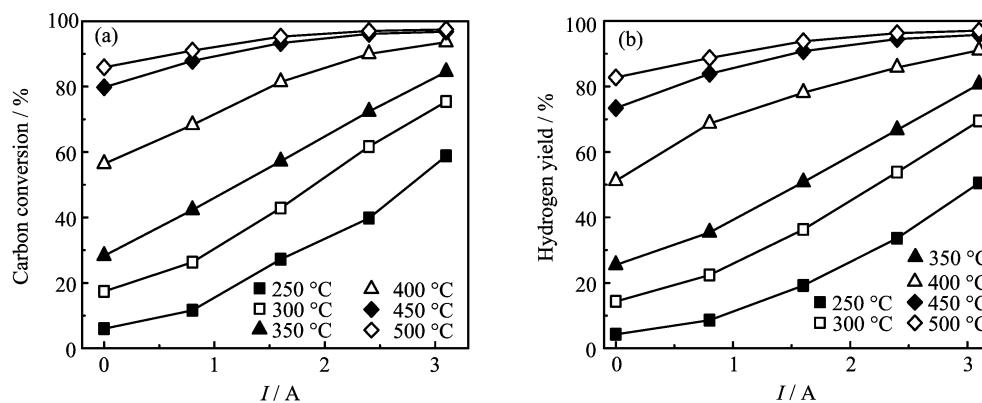


FIG. 3 Effect of the current on (a) the carbon conversion and (b) the hydrogen yield, measured as a function of current over the Cat V at different fixed temperatures, other reforming conditions:  $GHSV=10500$  h<sup>-1</sup>,  $S/C=6.9$ , and  $P=111.1$  kPa.

with the current increasing from 0 A to 3.1 A at the same temperature of 350 °C, and reached nearly complete conversion (96.8%) at 3.1 A and 450 °C. Figure 3(b) shows dependence of the hydrogen yield on current at given temperature. It was observed that the hydrogen yield was also promoted by the current.

Figure 4 depicts the influence of the current on the composition of the gaseous products over the NiCuMgCeAl catalyst. Hydrogen (about 62%–76%)

and carbon dioxide (21%–29%) are the major products together with smaller amount by-products of carbon monoxide (2%–4%) and a trace amount of methane (<4%). It was found that the concentrations of H<sub>2</sub> and CO slightly increased with the current increasing, accompanied by a decrease of concentrations of CO<sub>2</sub> and CH<sub>4</sub>. The above results indicated that the production of hydrogen from the bio-oil reforming can be realized at low-temperature using the multiple metal

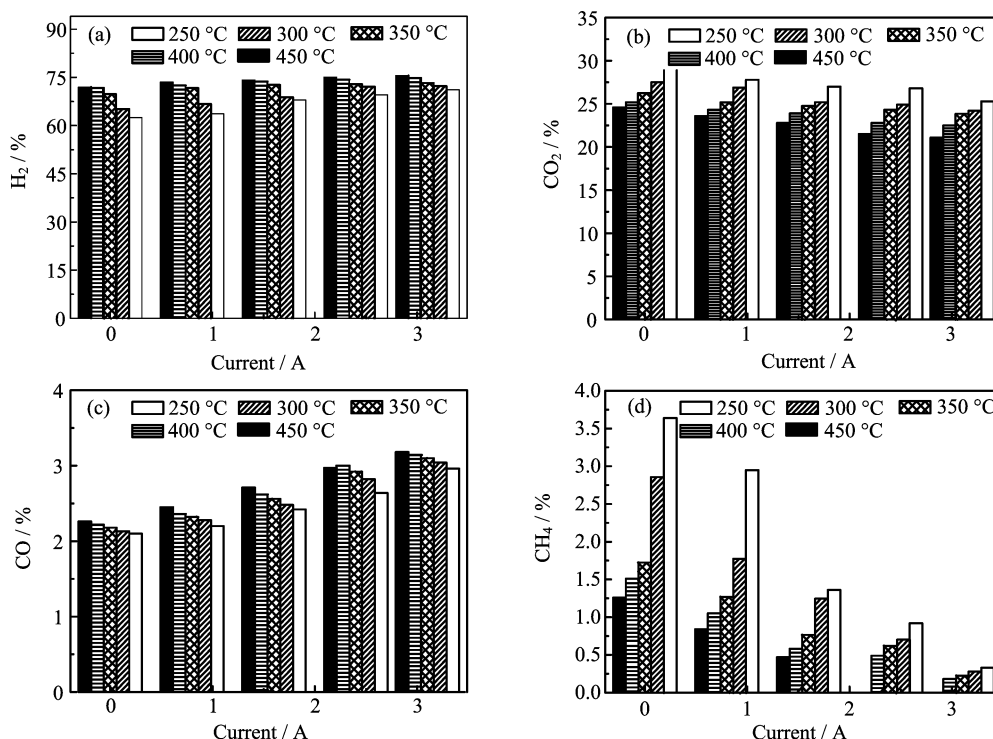


FIG. 4 The effect of the current on the distribution of the gas products for the bio-oil reforming over the Cat V. (a) The volume percentage of  $H_2$ , (b) the volume percentage of  $CO_2$ , (c) the volume percentage of  $CO$ , and (d) the volume percentage of  $CH_4$ , respectively. Reforming conditions:  $T=250\text{--}450\text{ }^\circ\text{C}$ ,  $GHSV=10500\text{ h}^{-1}$ ,  $S/C=6.9$ , and  $P=111.1\text{ kPa}$ .

doped Ni based catalyst and the ECR approach. This suggests that the researched catalyst may be one of most suitable candidates for the bio-oil reforming because this non-noble metal catalyst can efficiently reform the bio-oil to rich  $H_2$  and  $CO_2$  at low operating temperature ( $350\text{--}450\text{ }^\circ\text{C}$ ), being much lower than that using the conventional NiO-based catalysts ( $600\text{--}850\text{ }^\circ\text{C}$ ). The carbon conversion of the bio-oil using the  $18\%\text{NiO}/\text{Al}_2\text{O}_3$  catalyst was very low (about 14.7%) at  $400\text{ }^\circ\text{C}$  and only about 60% even at  $600\text{ }^\circ\text{C}$ . Even using ECR method, achieving 90% hydrogen yield should perform at  $550\text{--}600\text{ }^\circ\text{C}$  using Ni- $\text{Al}_2\text{O}_3$  catalyst [19]. However, it is possible to produce hydrogen from the bio-oil with high carbon conversion ( $>90\%$ ) and hydrogen yield ( $>90\%$ ) at low reforming temperature by using the ECR method over the researched catalyst. Lower operating temperature using the researched catalyst in the bio-oil reforming would be attributed to higher activity for the bio-oil reforming reactions. The decomposition of the oxygenated organic compounds and the water-gas shift reaction over this catalyst would be described in the next sections.

Moreover, the stability of the catalyst in the bio-oil reforming was tested by measuring the carbon conversion, the yield of hydrogen and the changes of the products compositions as a function of the time on stream. As shown in Fig.5, no obvious changes in the carbon conversion, the yield of hydrogen and the products dis-

tribution were observed for about the initial 15 h under typical reforming conditions ( $I=3.1\text{ A}$ ,  $T=400\text{ }^\circ\text{C}$ ,  $GHSV=10500\text{ h}^{-1}$ ,  $S/C=6.9$ , and  $P=111.1\text{ kPa}$ ). A slight decrease of the catalytic activity was observed for a longer term test. For example, the hydrogen yield gradually decreased by about 10% (from about 91% to 81%) for 30 h reforming, and the carbon conversion slightly decreased from about 95% to 88% (Fig.5(a)). As can be seen from Fig.5(b), the composition alteration of the products seems to be trivial during the investigated duration. The comparison of the activity and stability of selected catalysts in hydrogen production from steam reforming of bio-oil is shown in Table II. It is noticed that the catalyst inactivity of the Ni-based catalyst and other catalyst in the bio-oil reforming is much more serious as compared with present catalyst, which would be mainly attributed to lower carbon-deposition over the researched catalyst.

### C. Decomposition of acetic acid-model compound of bio-oil over the researched catalyst

The reaction pathways in the bio-oil steam reforming process are very complex, a lot of potential intermediates and products may be formed. The reaction network may consist of a complex set of numerous reactions with multiple pathways depending on the bio-oil used and the catalyst selected and the operating conditions. At

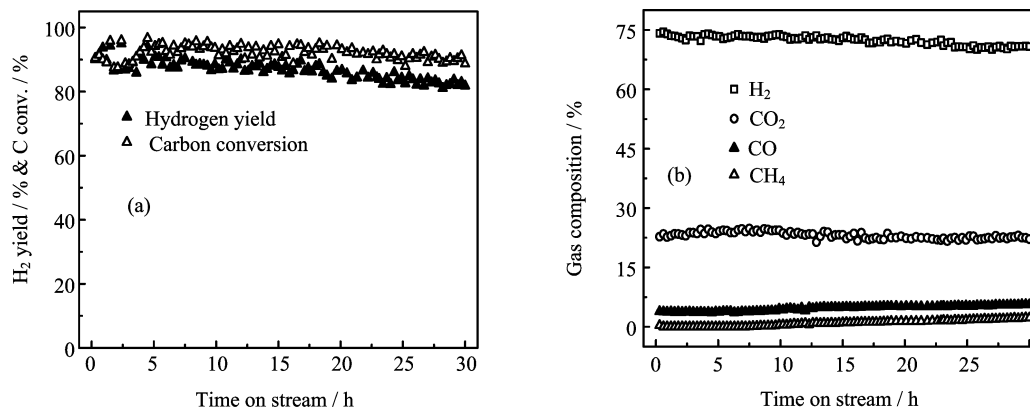


FIG. 5 Stability of the Cat V during the bio-oil reforming ( $T=400\text{ }^{\circ}\text{C}$ ,  $I=3.1\text{ A}$ ,  $\text{GHSV}=10500\text{ h}^{-1}$ ,  $S/C=6.9$ ,  $P=111.1\text{ kPa}$ ). (a) The hydrogen yield and carbon conversion and (b) the gaseous products composition.

TABLE II Comparison of activity and stability using the selected catalysts for hydrogen production from reforming of bio-oil.

| Catalyst  | Main operating condition |              |       |                             | Maximum value                |                          | Stability*   |
|---|--------------------------|--------------|-------|-----------------------------|------------------------------|--------------------------|--------------|
|   | $T/^{\circ}\text{C}$     | $I/\text{A}$ | $S/C$ | $\text{GHSV}/\text{h}^{-1}$ | $\text{H}_2\text{ yield}/\%$ | $\text{Carbon conv.}/\%$ |              |
| NiO-Al <sub>2</sub> O <sub>3</sub> [23]                                       | 825                      | 0            | 4.9   | 126000                      | 90                           | —                        | About 15 min |
| NiO-Al <sub>2</sub> O <sub>3</sub> [19]                                       | 600                      | 0            | 5.8   | 6048                        | 52.7                         | 65.4                     | —            |
| Ni-Co/MgO-La <sub>2</sub> O <sub>3</sub> -Al <sub>2</sub> O <sub>3</sub> [23] | 825                      | 0            | 4.9   | 126000                      | 90                           | —                        | About 30 min |
| 12%Ni/ $\gamma$ -Al <sub>2</sub> O <sub>3</sub> [29]                          | 850                      | 0            | 6.0   | 26000                       | 97.0                         | 71.5                     | —            |
| C12A7 [18]  | 750                      | 0            | 4.0   | 10000                       | 20                           | 35                       | —            |
| C12A7-O <sup>-</sup> /18%Mg [18]  | 750                      | 0            | 4.0   | 10000                       | 80                           | 95                       | About 3 h    |
| Pt/CeZrO <sub>2</sub> [30]  | 795                      | 0            | 10.8  | 3090                        | 65                           | —                        | —            |
| 1%Pt/ $\gamma$ -Al <sub>2</sub> O <sub>3</sub> [29]                           | 700                      | 0            | 6.0   | 26000                       | 98.3                         | 75.0                     | —            |
| Ni-Cu-Mg-Ce-Al  | 500                      | 0            | 6.9   | 10500                       | 82.8                         | 85.9                     | —            |
|   | 450                      | 3.1          | 6.9   | 10500                       | 95.8                         | 96.8                     | —            |
|   | 400                      | 3.1          | 6.9   | 10500                       | 91                           | 94                       | About 30 h   |

\* The stability refers to the duration once the H<sub>2</sub> yield decreases to the initial values of 50%.

least three different types reactions should be considered: (i) the steam reforming of the oxygenated organic compounds ( $\text{C}_n\text{H}_m\text{O}_k$ ) in the bio-oil (Eq.(1)), (ii) the decomposition of the oxygenated organic compounds ( $\text{C}_n\text{H}_m\text{O}_k \rightarrow \text{C}_x\text{H}_y\text{O}_z + \text{other fragments or gaseous small molecules}$ ), and (iii) the WGS reaction.

To further reveal the reaction of bio-oil reforming over the researched catalyst and to avoid the influence of water on the decomposition of the bio-oil, because the crude bio-oil and the pretreated one contained about 20%–40% H<sub>2</sub>O [19], we selected the acetic acid as the model compound and studied on the thermal decomposition over the researched catalyst. As shown in Fig.6, at temperature lower than 300 °C in the CSR, the conversion of the acetic acid decomposition was very low (<18%). With increasing temperature from 300 °C to 600 °C, the conversion of the acetic acid remarkably increased from about 18% to 68% without the current increase (Fig.6(a)). The conversion of the acetic acid increased from 21.3% to 56.8% with the current increasing

from 0 A to 2.0 A at 400 °C, and the hydrogen yield simultaneously increased with increasing of temperature and current (Fig.6 (a) and (c)). Main dry gas products from the acetic acid decomposition observed are H<sub>2</sub>, CO, CO<sub>2</sub>, CH<sub>4</sub>, and other hydrocarbons (C<sub>2</sub> and C<sub>2</sub><sup>+</sup> hydrocarbons *etc.*) (Fig.6 (b) and (d)). The composition of H<sub>2</sub> slightly increased with increasing temperature and current. When the temperature increased from 300 °C to 400 °C at the current of 2 A, the content of CO decreased from 10.8% to 9.7%, while the content of methane increased from 7.4% to 22.2%, subsequently with temperature increasing, the content of CO began to increase, while the content of methane kept slightly increase until to 500 °C then began to decrease, when the temperature increased to 600 °C, the content of CO reached 22.9%, while the content of methane decreased to 11.5%, however during the whole range of temperature increasing, the CO<sub>2</sub> content kept decreasing. The other hydrocarbons (C<sub>2</sub> and C<sub>2</sub><sup>+</sup> hydrocarbons *etc.*) kept decreasing with increasing temperature

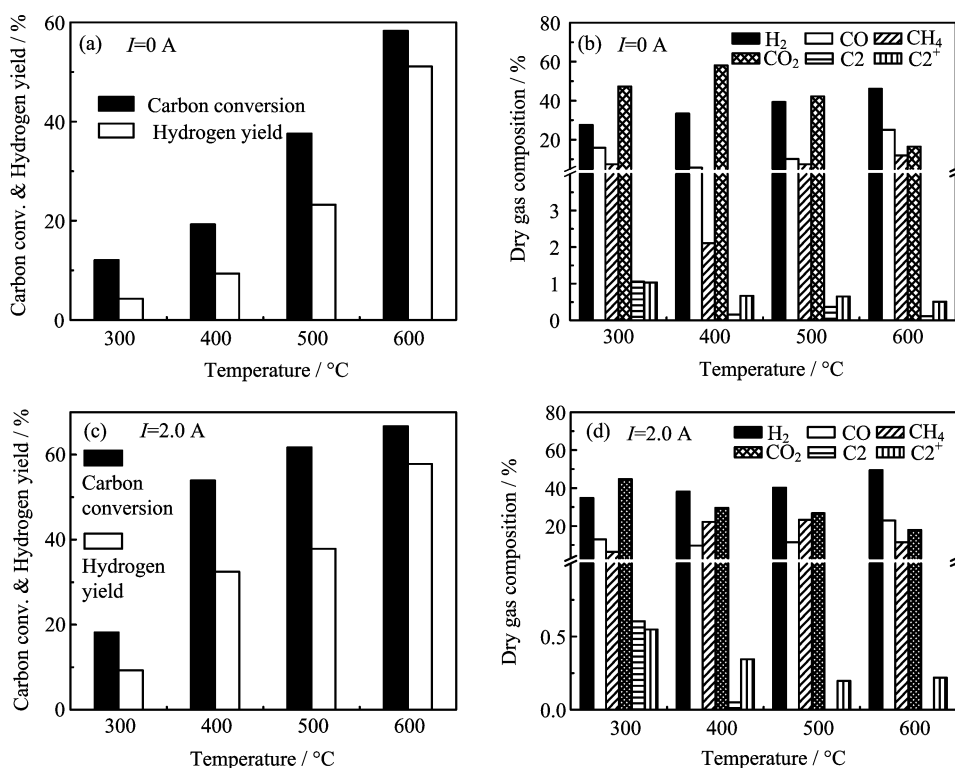
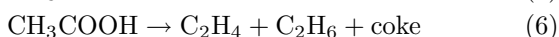
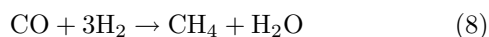


FIG. 6 The decomposition of the model compounds of bio-oil (acetic acid) over the researched catalyst. The effect of temperature on: (a) carbon conversion and hydrogen yield,  $I=0$  A, (b) the composition of the gaseous products,  $I=0$  A, (c) carbon conversion and hydrogen yield,  $I=2.0$  A, (d) the composition of the gaseous products from the decomposition of acetic acid,  $I=2.0$  A, respectively. Other conditions:  $T_{\text{decomposition}}=300\text{--}600$  °C, flow  $f(\text{Ar})=108$  mL/min, flow  $f(\text{acetic acid})=0.2$  mL/min, GHSV=5000  $\text{h}^{-1}$ , and  $P=111.1$  kPa.

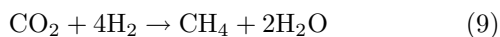
and current. From a mechanistic viewpoint, the overall reactions system involved in acetic acid decomposition is very complex. The main reactions can take place, according to the following reactions including decomposition (Eq.(4)–(Eq.6)) and Ketonization (Eq.(7))



In addition, we deduced that methane can also be formed by the hydrogenation of  $\text{CO}_x$  that is the methanation reaction [21]



$$\Delta H_{298} = -205.9 \text{ kJ/mol}$$



$$\Delta H_{298} = -112.9 \text{ kJ/mol}$$

which was in the following water-gas shift (WGS) experiments, we did observe hydrogenation of CO over the researched catalyst). The above results indicated that the catalyst efficiently dissociates the oxygenated organic compounds in the bio-oil over 300 °C.

#### D. Water-gas shift activity of researched catalyst

The WGS reaction (Eq.(2)) is a very important side reaction that affects the equilibrium of both CO and  $\text{CO}_2$  in the reforming of bio-oil. The WGS reaction is an encouraged elementary step for the reforming of bio-oil, for that it can enhance the hydrogen yield. To investigate the WGS activity over the researched catalyst, the conversion of CO to  $\text{CO}_2$  was tested using a model mixture of  $\text{CO}/\text{Ar}/\text{H}_2\text{O}$  (1:2:5.2 in mole ratio) corresponding to the reforming process within the temperature range of interest. As shown in Fig.7, the conversion of CO increases with increasing temperature at low temperature (<400 °C), reaching a near complete conversion (about 94.2%) at 400 °C. Further increasing temperature over 450 °C will lead to a decrease of the CO conversion. CO was mainly converted into  $\text{CO}_2$  with a selectivity of 99.2%–100% through the WGS reaction (Eq.(2),  $\Delta H_{298}=-41.1$  kJ/mol), accompanied by the formation of a trace amount of methane around 450 °C through the methanation reaction (Eq.(8),  $\text{H}_2$  was produced by WGS). The above experimental results suggests that the researched catalyst shows very high activity in WGS reaction in the range of 300–600 °C, which agreed with the results that the CO content in the final products gases is much lower than that of  $\text{CO}_2$

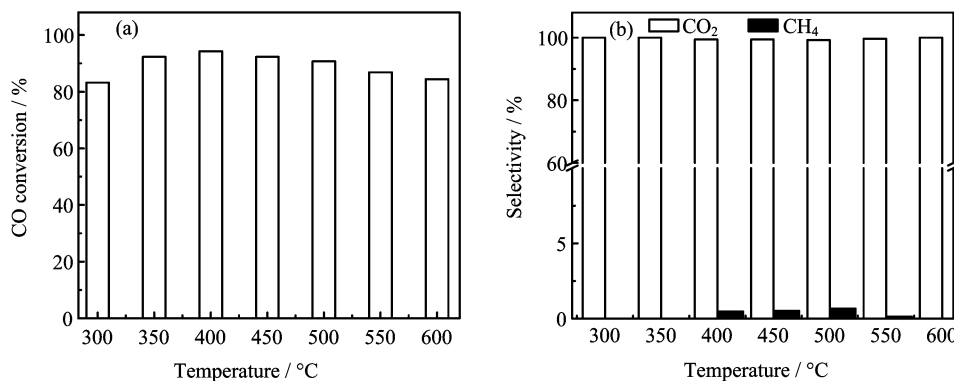


FIG. 7 WGS activity over the Cat-V. (a) CO conversion, (b) the selectivity to CO<sub>2</sub> and CH<sub>4</sub>, Other reaction conditions:  $I=0$  A, CO/Ar=1:2 (volume ratio),  $f(\text{CO}+\text{Ar})=120$  mL/min,  $f(\text{H}_2\text{O})=0.15$  mL/min,  $T_{\text{reforming}}=300-600$  °C, S/C=6.0, GHSV=5000 h<sup>-1</sup>, and  $P=111.1$  kPa.

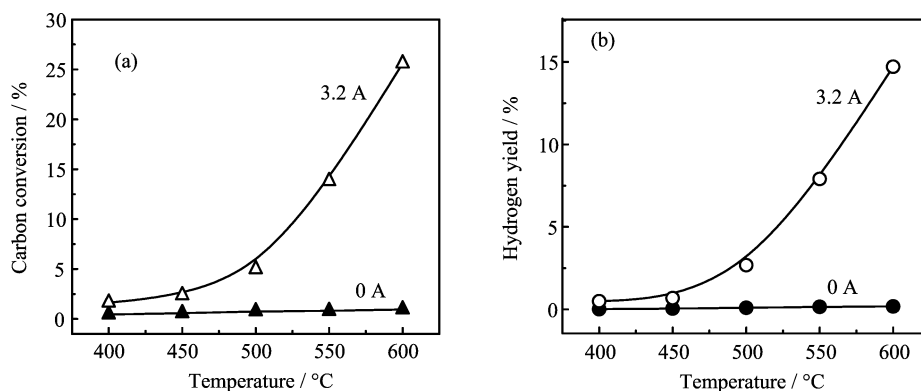


FIG. 8 The effect of the current on the decomposition of bio-oil via the homogeneous experiments through the quartz bed in the absence of any catalyst. (a) The carbon conversion, (b) the hydrogen yield. Other conditions:  $f_{\text{bio-oil}}=0.74$  mL/min,  $f_{\text{Ar}}=210$  mL/min, GHSV=6000 h<sup>-1</sup>, and  $P=111.1$  kPa.

from the bio-oil reforming (Fig.4).

### E. Effect of current on the thermal decomposition of bio-oil

The influence of current on the decomposition of bio-oil under 111 kPa was tested via the homogeneous experiments with and without the current through the quartz bed in the absence of any catalyst. As shown in Fig.8(a), the bio-oil conversion for the decomposition of bio-oil depends on both the temperature and the current. Without the current supplied (*i.e.*,  $I=0$  A), the carbon conversion was very low (about 8%) at 600 °C. However, the carbon conversion increased to 34.6% at the same temperature with current increasing to 3.2 A. It was also observed that the hydrogen yield was enhanced by the current (Fig.8(b)).

To further study the dissociation and reforming processes, the species desorbed from the catalyst surface were detected by an anionic TOF mass spectrometry under the low-pressure (0.1 Pa) using ethanol as a model compound of bio-oil for simplifying the reaction

system. Without the current supplied to the catalyst, no ionic signal was observed. When the current passed through the catalyst in Ar, only one peak near the mass number of zero was observed (Fig.9(a)), corresponding to the thermal electrons desorbed from the electrified Ni-Cr wire through the catalyst bed. The number density of thermal electrons flowing through the catalyst bed was about  $8.0 \times 10^8$  cm<sup>-3</sup> at 480 °C and  $I_{\text{Ni-Cr}}=3.2$  A, which was measured by a columned Au-coated Faraday-plate and an amperometer (Keithley model 6485). When a mixture gas of ethanol and argon was fed onto the electrified catalyst, a series of peaks appeared in the TOF spectrum (Fig.9(b)), corresponding to e<sup>-</sup>, H<sup>-</sup>, CH<sub>x</sub><sup>-</sup> ( $x=0-4$ ), OH<sup>-</sup>, and C<sub>2</sub>H<sub>x</sub><sup>-</sup> ( $x=0-5$ ), respectively. The ionic fragments of the hydrocarbons (CH<sub>x</sub><sup>-</sup>) and C<sub>2</sub>H<sub>x</sub><sup>-</sup> ( $x=0-5$ ) may form through the dissociation of ethanol by the thermal electrons on the catalyst surface (*i.e.*,  $e^-(s)+\text{C}_2\text{H}_5\text{OH}(s)\rightarrow\text{CH}_x^-(s)+\text{C}_2\text{H}_x^-(s)+\text{OH}^-(s)+\text{H}^-(s)\dots$ ; In addition, when a mixture of ethanol/water/argon was fed onto the electrified catalyst, the CO<sub>2</sub><sup>-</sup> peak was obviously observed (Fig.9(c)), which may arise from the ethanol reforming

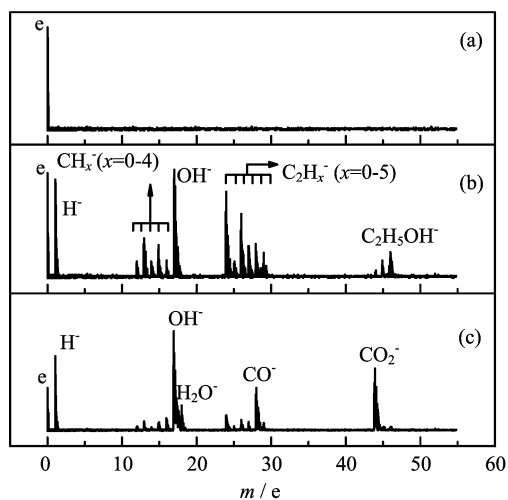


FIG. 9 Typical TOF spectra for (a) the current passed through the Cat V in argon ( $I=3.2$  A,  $T=575$  °C,  $P(\text{Ar})=0.27$  Pa), (b) the  $\text{C}_2\text{H}_5\text{OH}/\text{Ar}$  mixture fed onto electrified catalyst ( $I=3.2$  A,  $T=575$  °C,  $P(\text{C}_2\text{H}_5\text{OH})=0.06$  Pa,  $P(\text{Ar})=0.02$  Pa), (c) the mixture of  $\text{C}_2\text{H}_5\text{OH}/\text{H}_2\text{O}/\text{Ar}$  fed onto the electrified catalyst ( $I=3.1$  A,  $T=580$  °C,  $P(\text{H}_2\text{O})=0.14$  Pa,  $P(\text{Ar})=0.1$  Pa).  $P(\text{C}_2\text{H}_5\text{OH})=0.05$  Pa.

and the electron attachment processes. The above TOF results indicated that the thermal electrons desorbed from the electrified Ni-Cr wire in the catalyst bed and participated in the reforming and dissociation of the oxygenated organic compound.

#### F. Influence of current on catalyst properties

The features and alterations of the catalysts after CSR and ECR of the bio-oil were investigated by XRD, XPS, and BET analyses. Figure 10 shows typical XRD spectrum for four different researched catalyst samples. For the fresh catalyst (Fig.10(a)), the diffraction of peak was not obvious and the half width of the diffraction peak are all broad, it is indicating that the species are in high dispersive and amorphous state in the fresh catalyst. The diffraction profile at  $43.3^\circ$  corresponds to the oxide species of nickel (NiO). However, the XRD patterns for the used catalyst after the CSR and ECR are quite different from that of the fresh one. As shown in Fig.10(b), some sharp peaks appeared for the used ones, corresponding to the metallic phases  $\text{M}^0$  (*i.e.*, Ni<sup>0</sup> and Cu<sup>0</sup>). This means that the oxide states were reduced into the metallic states during the bio-oil reforming process. The reduction of the oxide states is mainly attributed to the reduction by hydrogen formed in the reforming of bio-oil (*i.e.*,  $\text{M}^{2+} + \text{H}_2 \rightarrow \text{M}^0$ ). Especially, the intensity of the diffraction peaks became stronger after the ECR (Fig.10(c)), as compared with those after the CSR (Fig.10(b)). One of possible explanation is that a part of the oxide states were reduced into the metallic states by the thermal electrons (*i.e.*,  $\text{M}^{2+} + 2\text{e}^- \rightarrow \text{M}^0$ )

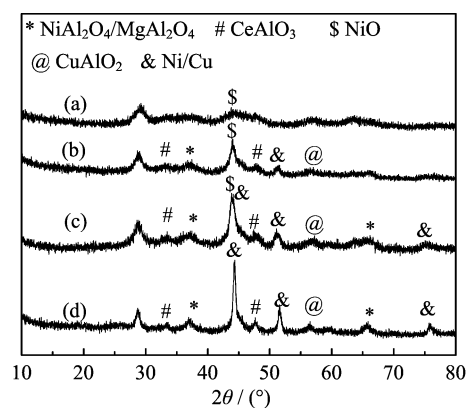


FIG. 10 Typical XRD spectra of the Cat V catalyst. (a) the fresh catalyst prepared, (b) the used one after CSR at  $400$  °C for 4 h, (c) the used one after ECR at  $400$  °C and  $3.1$  A for 4 h, and (d) the used one after ECR at  $400$  °C and  $3.1$  A for 30 h, respectively.

during the ECR process. This explanation would be supported by the following experimental observations: (i) the desorption of the thermal electrons from the electrified catalyst was directly observed by the TOF measurements (Fig.9) and (ii) the reduction from the oxidation state to the metallic phase also occurred when a current passed through the catalyst in Ar or He [19].

Moreover, the alterations of the atomic states on the catalyst surface after the ECR reforming of bio-oil were further investigated by the XPS measurements. As shown in Fig.11(A), the bind energy at about 855.9 and 862.1 eV were observed for the fresh catalyst, which were assigned to the main line of Ni<sup>2+</sup>(2p<sub>3/2</sub>) and its satellite, respectively [22]. After the ECR reforming, a new peak near 852.7 eV was observed in the Ni XPS spectrum, corresponding to the peak of the metallic Ni<sup>0</sup>(2p<sub>3/2</sub>). The above results clearly showed that Ni was in +2 “formal” oxidation states in the fresh catalyst and part of Ni<sup>2+</sup> (*i.e.*, the NiO phase) was reduced to metallic Ni<sup>0</sup> after the ECR reforming of bio-oil at  $400$  °C after 30 h. Figure 11(B) displays the Cu XPS spectra (930–970 eV) from the samples mentioned above. The reduction from +2 “formal” oxidation states of Cu<sup>2+</sup>(2p<sub>3/2</sub>) (933.8 eV) into the metallic Cu<sup>0</sup>(2p<sub>3/2</sub>) (932.7 eV) were also identified after the reforming of bio-oil, but no obvious reduction was found for the oxidation states of Ce<sup>2+</sup> and Mg<sup>2+</sup> under the reforming of the bio-oil at  $400$  °C. In addition, the BET surface areas and pore volume were also measured for the samples mentioned above (Table III). In comparison with the fresh catalyst, the BET surface areas, pore volume and pore diameter from the used ones after the reforming slightly decreased, but compared with the used one after CSR, the pore diameter of the catalyst after the ECR slightly increased. Generally, the decrease of the BET surface area will lead to the decrease of the catalyst activity. However, it was observed that the current

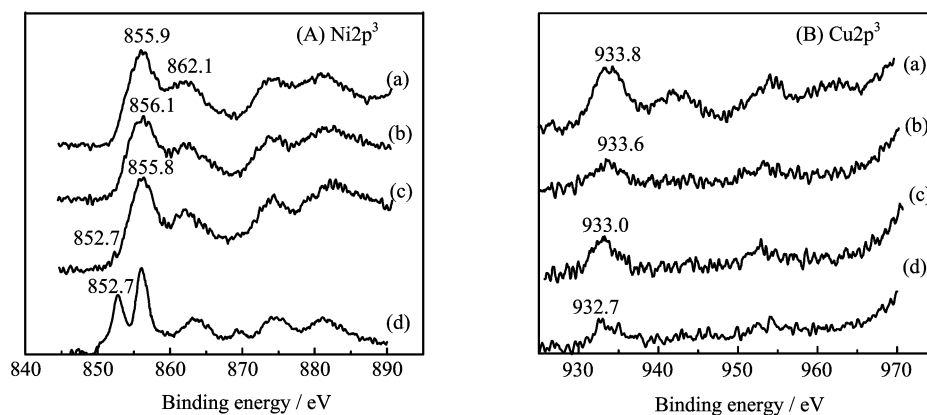


FIG. 11 The Ni/Cu XPS spectra of the Cat V catalyst. (a) The fresh prepared, (b) the used one after CSR at 400 °C for 4 h, (c) the used one after ECR at 400 °C and 3.1 A for 4 h, and (d) the used one after ECR at 400 °C and 3.1 A for 30 h, respectively.

TABLE III Characteristic alteration of Cat V before and after the bio-oil reforming (BET in m<sup>2</sup>/g, pore volume in cm<sup>3</sup>/g, and pore diameter in nm).

| Sample* | BET   | Pore volume | Pore diameter |
|---------|-------|-------------|---------------|
| No.1    | 205.1 | 0.66        | 12.8          |
| No.2    | 198.9 | 0.56        | 11.4          |
| No.3    | 195.2 | 0.55        | 11.6          |
| No.4    | 191.3 | 0.55        | 11.9          |

\* No.1: the fresh researched catalyst. No.2: the catalyst after the common steam reforming at  $T=400$  °C for 4 h. No.3: the catalyst after electrochemical chemical catalytic steam reforming at  $T=400$  °C,  $I=3.1$  A, for 4 h. No.4: the catalyst after electrochemical chemical catalytic steam reforming at  $T=400$  °C,  $I=3.1$  A, for 30 h.

supplied in ECR obviously promoted the production of hydrogen from bio-oil. The above results may indicate that, the alterations of the catalyst properties induced by the current would have a minor influence on the production of hydrogen from the electrochemical catalytic reforming of the bio-oil.

## G. Discussion

The researched catalyst shows good activity and long lifetime for the bio-oil reforming at low temperature. Low operating temperature in the bio-oil reforming would be attributed to high activity of the researched catalyst for the bio-oil reforming reactions, the decomposition of the oxygenated organic compounds, the water-gas shift reaction. In the researched catalyst, the element of Ni is a very composition for the reforming reactions, and meanwhile, may play an important role in promoting C–C or C–H bonds rupture of oxygenated organic compounds in the bio-oil. Even though the compositions of Cu/Ce/Mg have a lower reforming ac-

tivity (Fig.2), they significantly enhance the activity of the WGS reaction, leading to an increase of the hydrogen yield (Fig.3 and Fig.7). In addition, the lifetime of the catalyst in the bio-oil reforming (Fig.5) is also much longer than that of the other NiO-based catalyst [23]. Adding Ce and Mg to the reforming catalysts favors to reduce the carbon-formation and the congregation of active components during the bio-oil reforming.

Moreover, the performance of the bio-oil reforming was significantly promoted by the current through the catalyst during the ECR process of the bio-oil. In particular, the hydrogen yield significantly increased with increasing the current, accompanied by a decrease of the by-product of methane content (Fig.3 and Fig.4). Several factors should be considered to account for the current effects, as mentioned below.

Firstly, the current enhanced the decomposition of the oxygenated organic compounds ( $C_nH_mO_k$ ) in the bio-oil. Bio-oil contains numerous and complex oxygenated organic compounds including acids, alcohols, aldehydes, ketones, substituted phenolics, and other oxygenates. Hydrogen can be directly produced by the decomposition of acetic acid, one main oxygenated organic compound in the bio-oil (Fig.6). And ethanol, the other important organic compound in the bio-oil, also can be decomposed to produce hydrogen [16]. In addition, the decomposition can form a series of the intermediates such as H, OH, and CH *etc.* The intermediates may readily react with other organic compounds and/or water, speeding up the reforming reactions and/or further decomposition.

Secondly, the thermal electrons, originating from the electrified wire, promoted the decomposition and reforming of the bio-oil in the ECR process. The presence of the thermal electrons both on the electrified Ni-Cr wire and on the electrified catalyst surface was directly observed by the anionic TOF measurements (Fig.9). It is well known that when an electrified metal or a metal oxide is heated, electrons can boil off its surface, lead-

ing to thermal electrons emission from surface [24]. It has been reported that thermal electrons on a metal or metal oxide surface play an important role in the reduction process (*e.g.*,  $O_2 + 4e^- \rightarrow 2O^{2-}$ ) [25] and in the molecular decomposition or ionization processes. Small molecular dissociation of  $O_2$ ,  $H_2$ ,  $F_2$ ,  $H_2O$  and  $C_6H_6$  via the thermal electrons has also been observed on the Ca-Al-O oxides surface [20, 26–28]. The promoting effect of the current on the molecular decomposition, the reforming, and the catalyst reduction is supported by the following observations: (i) presence of the thermal electrons both on the electrified Ni-Cr wire and on the electrified catalyst surface was directly observed by the anionic TOF measurements (Fig.9(a)), (ii) the dissociation of the oxygenated organic compound (ethanol as a model) into the hydrocarbon fragments ( $CH_x$ ) and the dissociation of water into OH by the thermal electrons on the electrified catalyst surface were also observed (Fig.9(b)). (iii) An additional reduction from the oxidation state to the metallic phase in the catalyst was observed when a current passed through the catalyst, which is being attributed to the reaction of  $M^{2+}$  with the thermal electrons (*e.g.*,  $Ni^{2+} + 2e^- \rightarrow Ni^0$ ) (Fig.10). Accordingly, the thermal electrons may play an important role in promoting the bio-oil decomposition, its reforming and the catalyst reduction, partly leading to the increase of the hydrogen yield during the ECR process.

Thirdly, it was also noticed that the ECR and CSR processes have different temperature distribution in the catalyst bed [19]. The maximal temperature gradients in ECR process were higher than those in CSR. Even though temperature in the center of the catalyst bed is almost close to the average value in our investigated range (250–550 °C), the local temperature on the surface of the electrified Ni-Cr wire or near the wire, generally, was obviously higher than the average temperature. Accordingly, the activity of the catalyst reforming near the electrified Ni-Cr wire should be higher than that of other positions in the bed, partly, leading to an increase of the overlap hydrogen yield during the ECR process.

In a word, the high efficient production of hydrogen from low-temperature reforming of bio-oil would be attributed to the higher activity of the mixed oxide catalyst for the bio-oil reforming reactions, the decomposition of the oxygenated organic compounds of bio-oil, the water-gas shift reaction and the current promoting effects on the decomposition and reforming of the bio-oil in the ECR process.

#### IV. CONCLUSION

We studied a new multiple metal doped Ni based mixed oxide catalyst. It shows high efficient and long lifetime in production of hydrogen from low-temperature reforming of bio-oil. And the catalyst also

shows high activity for the decomposition of the oxygenated organic compounds of bio-oil and the water-gas shift reaction. Both the hydrogen yield and the carbon conversion reached over 90% at 400 °C in the ECR process. The hydrogen yield of 82.8% and carbon conversion of 85.9% were obtained in the CSR process at 500 °C during the bio-oil reforming. The performance of the bio-oil reforming is also significantly promoted by the current through the catalyst, accompanied by a decrease of the by-product of methane content during the ECR process of the bio-oil. The current through the catalyst bed provided abundant thermal electrons, enhanced the decomposition of the oxygenated organic compounds in the bio-oil and promoted the catalyst reduction. The mixed oxide catalyst developed would be one of most suitable candidates for the bio-oil reforming because this non-noble metal catalyst can efficiently reform the bio-oil to  $H_2$  (62%–76%) and  $CO_2$  (21%–29%) at lower operating temperature (250–500 °C) with a longer lifetime, as compared with conventional  $NiO-Al_2O_3$  catalysts (600–850 °C). The low-temperature reforming approach using the reforming researched catalyst and the ECR method, potentially, may be a useful route to practically produce  $H_2$  from bio-oil or other hydrocarbons.

#### V. ACKNOWLEDGEMENTS

This work is supported by the National Natural Science Foundation of China (No.51161140331), the National High Technology Research and Development of Ministry of Science and Technology of China (No.2013CB228105), and the Natural Science Research Project of Education Department of Anhui (No.kj2012Z330).

- [1] S. Ayalur Chattanathan, S. Adhikari, and N. Abdoulmoumine, *Renewable Sustainable Energy Rev.* **16**, 2366 (2012).
- [2] M. Y. Shpirt and N. P. Goryunova, *Solid Fuel Chem.* **43**, 378 (2009).
- [3] Y. Ishida, K. Kumabe, K. Hata, K. Tanifuji, T. Hasegawa, K. Kitagawa, N. Isu, Y. Funahashi, and T. Asai, *Biomass Bioenergy* **33**, 8 (2009).
- [4] D. N. Wang, S. Czernik, and E. Chornet, *Energy Fuels* **12**, 19 (1998).
- [5] T. J. Chen, C. Wu, and R. H. Liu, *Bioresour. Technol.* **102**, 9236 (2011).
- [6] F. Xu, Y. Xu, H. Yin, X. F. Zhu, and Q. X. Guo, *Energy Fuels* **23**, 1775 (2009).
- [7] S. Czernik, R. French, C. Feik, and E. Chornet, *Ind. Eng. Chem. Res.* **41**, 4209 (2002).
- [8] D. Wang, S. Czernik, D. Montane, M. Mann, and E. Chornet, *Ind. Eng. Chem. Res.* **36**, 1507 (1997).
- [9] X. Hu and G. X. Lu, *Appl. Catal. B* **88**, 376 (2009).

- [10] Y. Y. Wang, Y. L. Zhang, L. Meng, J. B. Wang, and W. Q. Zhang, *Biomass Bioenergy* **33**, 1131 (2009).
- [11] F. S. Azad, J. Abedi, E. Salehi, and T. Harding, *Chem. Eng. J.* **180**, 145 (2012).
- [12] G. Ozkan, S. Gok, and G. Ozkan, *Chem. Eng. J.* **171**, 1270 (2011).
- [13] M. Marquovich, S. Czernik, E. Chornet, and D. Montane, *Energy Fuels* **13**, 1160 (1999).
- [14] A. Bshish, Z. Yakoob, B. Narayanan, R. Ramakrishnan, and A. Ebshish, *Chem. Pap. Chem. Zvesti* **65**, 251 (2011).
- [15] S. Thaicharoensutcharittham, V. Meeyoo, B. Kitiyanan, P. Rangsunvigit, and T. Rirksomboon, *Catal. Today* **164**, 257 (2011).
- [16] L. X. Yuan, T. Q. Ye, F. Y. Gong, Q. X. Guo, Y. Torimoto, M. Yamamoto, and Q. X. Li, *Energy Fuels* **23**, 3103 (2009).
- [17] Y. Q. Chen, L. X. Yuan, T. Q. Ye, S. Q. Qiu, X. F. Zhu, Y. Torimoto, M. Yamamoto, and Q. X. Li, *Int. J. Hydrogen Energy* **34**, 1760 (2009).
- [18] Z. X. Wang, Y. Pan, T. Dong, X. F. Zhu, T. Kan, L. X. Yuan, Y. Torimoto, M. Sadakata, and Q. X. Li, *Appl. Catal. A* **320**, 24 (2007).
- [19] L. X. Yuan, Y. Q. Chen, C. F. Song, T. Q. Ye, Q. X. Guo, Q. S. Zhu, Y. Torimoto, and Q. X. Li, *Chem. Commun.* 5215 (2008).
- [20] F. Huang, J. Li, L. Wang, T. Dong, J. Tu, Y. Torimoto, M. Sadakata, and Q. X. Li, *J. Phys. Chem. B* **109**, 12032 (2005).
- [21] J. N. Park and E. W. McFarland, *J. Catal.* **266**, 92 (2009).
- [22] S. Velu, K. Suzuki, M. Vijayaraj, S. Barman, and C. S. Gopinath, *Appl. Catal. B* **55**, 287 (2005).
- [23] L. Garcia, R. French, S. Czernik, and E. Chornet, *Appl. Catal. A* **201**, 225 (2000).
- [24] G. A. Somorjai, *Introduction to Surface Chemistry and Catalysis*, New York: Wiley, 362 (1994).
- [25] W. Jamsak, S. Assabumrungrat, P. L. Douglas, N. Laosiripojana, R. Suwanwarangkul, S. Charojrochkul, and E. Croiset, *Chem. Eng. J.* **133**, 187 (2007).
- [26] C. F. Song, J. Q. Sun, S. B. Qiu, L. X. Yuan, J. Tu, Y. Torimoto, M. Sadakata, and Q. X. Li, *Chem. Mater.* **20**, 3473 (2008).
- [27] T. Dong, J. Li, F. Huang, L. Wang, J. Tu, Y. Torimoto, M. Sadakata, and Q. X. Li, *Chem. Commun.* 2724 (2005).
- [28] F. Huang, J. Li, L. Wang, S. Q. Yu, Y. Torimoto, M. Sadakata, and Q. X. Li, *Chem. Mater.* **17**, 2771 (2005).
- [29] X. Z. Wang, T. Dong, L. X. Yuan, T. Kan, X. F. Zhu, Y. Torimoto, M. Sadakata, and Q. X. Li, *Energy Fuels* **21**, 2421 (2007).
- [30] C. Rioche, S. Kulkarni, F. C. Meunier, J. P. Breen, and R. Burch, *Appl. Catal. B* **61**, 130 (2005).